ANALYZER FOR SPECTROSCOPY OF LOW-IMPEDANCE OBJECTS

Jerzy Hoja, Grzegorz Lentka

*Gdansk University of Technology, Faculty of Electronics Telecommunication and Informatics, Narutowicza 11/12, 80-952 Gdańsk, Poland
(✉ hoja@eti.pg.gda.pl, +48 58 347 1487; lentka@eti.pg.gda.pl)*

Abstract

The paper presents an analyzer making possible impedance measurements in the range of $1\ \Omega < |Z_x| \leq 100\ M\Omega$. New solutions of input circuitry and phase-sensitive detection technique of measurement signals were used. The input circuit was designed in the form of a 5-terminal measurement probe, which allows decreasing the influence of parasitic resistance, inductance and capacitance on the accuracy of impedance measurement in a wide frequency range from 1 mHz up to 10 MHz. The probe extracts two signals proportional to current through and voltage across the measured impedance. In order to determine orthogonal parts of the extracted measurement signals in a high frequency subrange $1\ MHz \div 10\ MHz$, the undersampling technique was used, allowing phase-sensitive detection using 12-bit ADCs with maximum sampling frequency equal to 10 MHz.

Keywords: impedance measurement, impedance spectroscopy, measurement probe, DSP.

1. Introduction

Impedance spectroscopy is counted to basic research methods for objects which are modeled by electrical circuits. It is used in different disciplines e. g. in electrochemistry [1], civil engineering [2], biology and medicine [3]. In order to identify parameters of equivalent circuits of such different objects using impedance spectroscopy, it is necessary to perform impedance measurements in a wide frequency range depending on the range of object's impedance change. In case of high-impedance objects ($|Z_x| \leq 100\ G\Omega$) the range of very low frequencies, even of the order of 100 μHz, is important, but for low-impedance objects ($|Z_x| \geq 1\ \Omega$) the high frequency range up to 10 MHz is required.

In the frame of European project Eureka E!3174, the authors have developed an analyzer for the spectroscopy of high-impedance objects (high-thickness anticorrosion coatings) [4]. The analyzer allows impedance measurements in a range of $1\ k\Omega < |Z_x| \leq 100\ G\Omega$ for frequencies in the range from 100 μHz up to

1 MHZ. Taking into account the requirements assumed for different objects, it was decided to extend the measurement parameters of the previously developed analyzer. Extensions apply to the measurement of low impedance (from 1 Ω) for the high-frequency part of the spectrum (up to 10 MHz). Application of new possibilities permit the use of new hardware and software solutions when comparing with the high-impedance analyzer.

The paper presents a new solution concerning the input circuitry and phase-sensitive detection of the measurement signals. The input circuitry was designed in the form of a 5-terminal measurement probe which allows decreasing the influence of parasitic resistance, inductance and capacitance on the error of impedance measurement in a wide frequency range from 1 mHz up to 10 MHz. The probe extracts two signals proportional to current through and voltage across the measured impedance. In order to determine orthogonal parts of the extracted measurement signals in a high frequency subrange 1 MHz $\div$ 10 MHz, the undersampling technique was used, allowing phase-sensitive detection using 12-bit ADCs with maximum sampling frequency equal to 10 MHz.

2. The architecture of the analyzer

In the high-impedance analyzer [5], the need of the measurements at very high impedance at very low frequencies leads to the solutions non-typical for conventional instrumentation for impedance measurement:

– The impedance measurement range up to $|Z_x| \leq 100$ GΩ has excluded the possibility of direct connection of Z_x to the input of the analyzer using shielded cables. The authors decided to use a high-impedance probe, which made possible a direct connection of the measured object to the input circuit.

– The use of the digital signal processing technique, which allows determination of orthogonal parts of the measurement signals at very low measurement frequencies down to 100 µHz.

The solution applied in the high-impedance analyzer allows to modify the analyzer architecture towards an analyzer for spectroscopy of low-impedance objects. The hardware changes concern only the measurement probe, but the software was changed for a CPLD programmable chip and DSP processor, in which the authors have implemented the method for determination of orthogonal parts of the measurement signals in the frequency range of 1 MHz $\div$ 10 MHz using the undersampling technique. The architecture of the realized analyser is shown in Fig. 1 emphasizing blocks realizing the new features of the analyser.
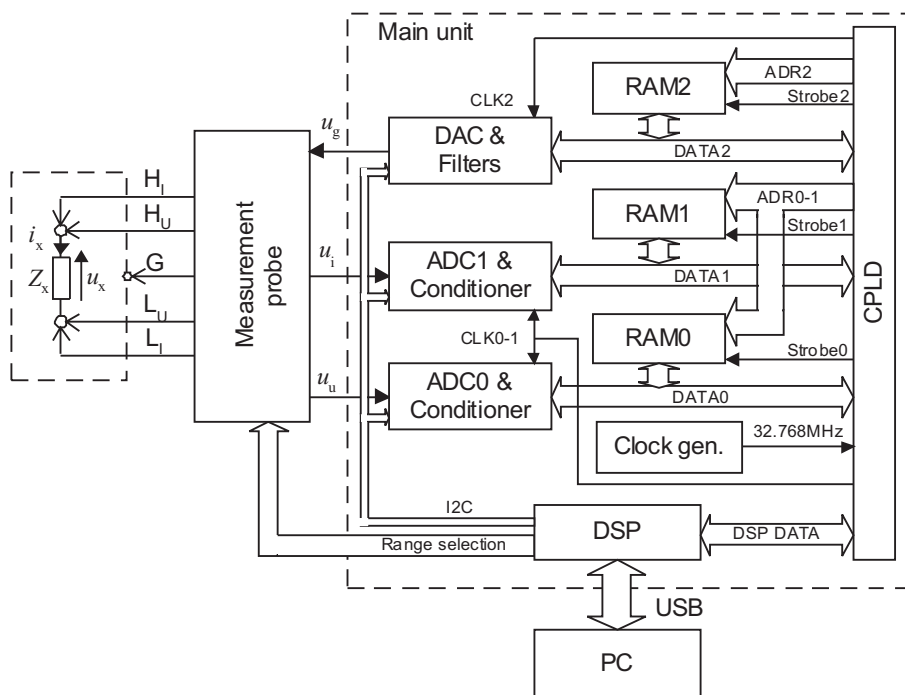
Fig. 1. Block diagram of the low-impedance analyzer.

The measured object is connected to the measurement probe to which the signal u_g is applied. The probe extracts two signals proportional to current through and voltage across the impedance Z_x, which can be used to determine the impedance on the basis of definition. The main unit of the analyzer contains the path for generation of the measurement signal u_g and two identical paths for processing signals extracted in the probe u_i and u_u. In the generation path, the sinusoidal signal is prepared using direct digital synthesis (DDS), with programmed frequency and amplitude. In the paths for processing signals u_i and u_u antialiasing filters and 12-bit ADCs were used.

On the basis of two sets of the samples of voltages u_i and u_u acquired in RAM memories, using DFT transformation, orthogonal parts of the measurement signals are determined. To assure simple calculation of DFT transformation, the CPLD program-mable circuit was used to allow synchronous generation of signal u_g (DAC strobing) and acquisition of the measurement signals with the aid of ADCs (two versions depending on the measurement frequency: below or above 1 MHz). Calculation of the orthogonal parts of signals u_i and u_u is performed by DSP after each measurement cycle. The DSP also calculates the modulus and argument of the measured impedance.
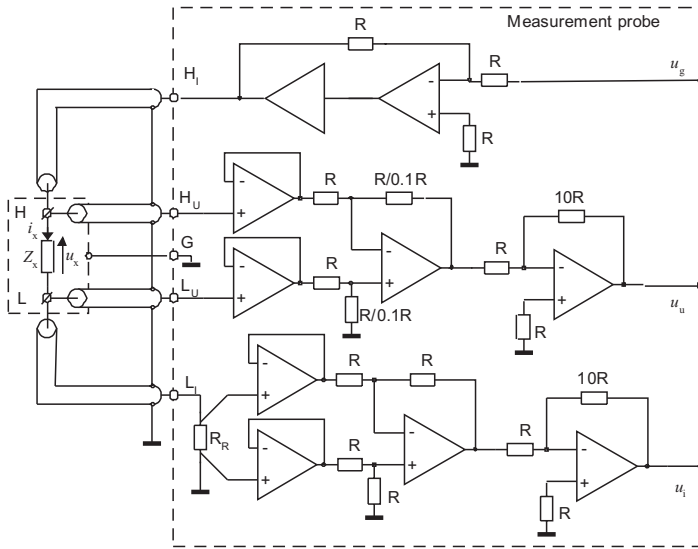
Fig. 2. Schematic diagram of the measurement probe.

Figure 2 presents a schematic diagram of the probe. It is the 5-terminal input circuitry (H_I, L_I – current terminals, H_U, L_U – voltage terminals, G – terminal for shielding of the measurement object), which allows to extract two signals proportional to current through $u_i \sim i_x$ and voltage across $u_u \sim u_x$ the impedance Z_x. The range resistor R_R connected in series with Z_x is used to measure current i_x flowing through Z_x. To assure a wide measurement range of the impedance Z_x (the measurement range of the current i_x changes from 10 nA up to 100 mA) the range resistor R_R is switched in decades (1 Ω, ...100 kΩ, 1 MΩ) by the miniature reed relays. The value of the range resistance R_R is selected in relation to $|Z_x|$ of the measured object according to the criterion: $0,01\ |Z_x| < R_R \leq 0,1\ |Z_x|$ (this condition is not fulfilled only at the lowest measurement range, because R_R does not change its value, but the maximum measurement voltage u_g is limited to 0,1 V). The fulfilment of the above condition means that resistance R_R is, at least, of an order lower than $|Z_x|$ and causes a ten-fold decrease of the impedance seen from terminal L in relation to the ground. This is a profitable solution due to lowering the influence of the capacitance of the shielded cables on the range resistors, but it arises the need of additional amplification ×10 of the signal from R_R. This way the amplitude of signal u_i is comparable to the amplitude of signal u_u, obtained from impedance Z_x.

In order to decrease the influence of the AC parameters of operational amplifiers in a wide range of the measurement frequency (1 mHz ÷ 10 MHz), both paths were realized in identical configuration, because this leads to compensation of identical phase shifts when determining impedance as a ratio of two signals u_u and u_i. In order

to limit the maximal measurement current to 100 mA, the range resistor $R_R = 1\ \Omega$ is used in two ranges: $1\ \Omega \div 10\ \Omega$ and $10\ \Omega \div 100\ \Omega$, but in the lowest range the resultant gain of the voltage across Z_x measurement path is increased to 10.

3. An analysis of the low-impedance probe

To perform an analysis of the influence of parasitic capacitance and inductance of the shielded cables and real-life parameters of the used OPAMPs on the extracted signals u_i and u_u, the equivalent circuit of the probe was proposed, as shown in Fig. 3.
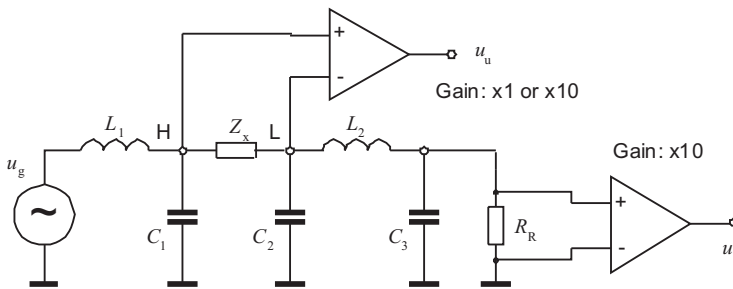

Fig. 3. Equivalent circuit of the measurement probe.

The equivalent circuit takes into account the following components:
L_1 and L_2 – inductance of the current cables connecting terminals H_I and L_I with terminals H and L, respectively,
C_1 – resulting capacitance seen from terminal H, introduced by cables connecting impedance Z_x to terminal H, layout capacitances inside the probe and the voltage-follower input capacitance,
C_2 – resulting capacitance seen from terminal L, introduced by analogous capacitances like in case of terminal H,
C_3 – capacitance resulting from capacitance of the shielded cable connected to terminal L_I, layout capacitances and capacitance entered by reed relays changing the measurement range, which are connected in parallel with R_R,

$$A_u = \frac{A_{DC}}{1 + j\frac{\omega}{\omega_{3dB}}}$$ – is the single-pole (ω_{3dB}) transfer function of amplifiers,

A_{DC} – open-loop *DC* gain of the amplifier [6].
On the basis of the assumed equivalent circuit of the probe, the formula determining the ratio U_u and U_i was elaborated:

$$\frac{U_u}{U_i} = Z_x \left(\frac{k_1}{1 + \frac{k_2}{A_u}} \right) \left(1 + \frac{2}{A_u} \right) \left[j\omega C_2 \left(j\omega L_2 + \frac{1}{j\omega C_3 + \frac{1}{R_R}} \right) + 1 \right] \left(j\omega C_3 + \frac{1}{R_R} \right), \quad (1)$$

where: $k_1 = 1$ and $k_2 = 2$ for range $1\ \Omega - 10\ \Omega$ (the gain in the voltage channel is equal to 10) and $k_1 = 0{,}1$ and $k_2 = 1{,}1$ for other ranges (the gain in the voltage channel is equal to 1).

It was assumed that the gain of the voltage followers is equal to 1 in the analyzed frequency range, because followers are realized using identical OPAMPs and the ratio of signals from both paths is calculated, so the elimination of gain errors takes place.

The analysis of the influence of the real-life components of the probe (on the basis of the formula (1)) on the error of the impedance measurement Z_x (relative error of $|Z_x|$ and absolute error of argument of Z_x) was performed in Matlab. It was done in two stages, in turn taking into account: parasitic capacitance and next parameters of the transfer function of OPAMPs and inductance of the cables.

3.1. Parasitic capacitances

The simulations were performed for three objects with impedance $Z_x = 10\ \text{k}\Omega$, $100\ \Omega$, $1\ \Omega$, using range resistors $R_R = 1\ \text{k}\Omega$, $10\ \Omega$ and $1\ \Omega$, respectively. The errors of modulus and argument Z_x were determined (Fig. 4) as a function of the measurement frequency for two values of capacitances C_2 and C_3: 10 pF and 30 pF.
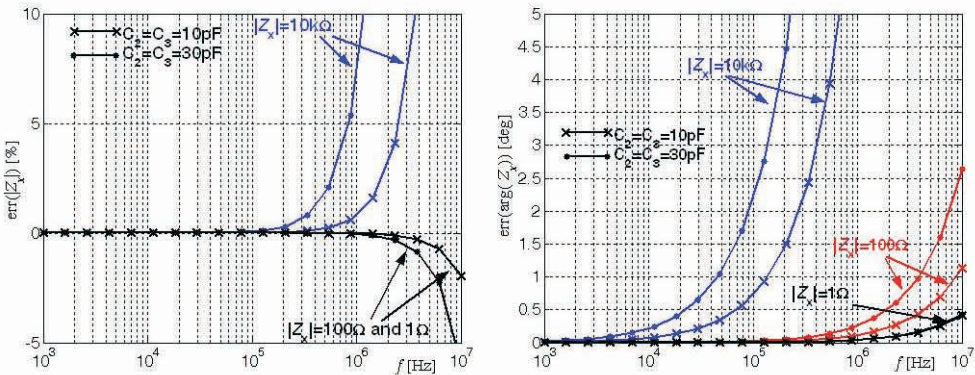

Fig. 4. Impedance modulus and argument measurement error caused by cable capacitance
for different ranges.

When analyzing the graphs, a fast increase of the errors can be noted for frequencies above 100 kHz for measured $Z_x = 10\ \text{k}\Omega$ and analogously ca. 1 MHz for

Z_x = 100 Ω. This error appears due to the resulting capacitance seen from terminal L, shunting the range resistor R_R and as a result causing erroneous measurement of the current i_x. Because decreasing the capacitance below several pF is difficult from a practical point of view (the most important is the capacitance of the cables), so the only way of decreasing the measurement error in this case is taking into account the real value of parasitic capacitance in formula determining the measured impedance. The resulting capacitance existing on terminal H does not affect the measurement error, but causes the decrease of the measurement signal on the impedance Z_x.

3.2. AC parameters of the operational amplifier and parasitic inductance

Due to the maximal value of the measured impedance $|Z_x|$= 100 MΩ the OPAMPs working as voltage followers in the probe must be characterized by low input currents (at the level of 10 pA) and small differential and common input capacitances (a few pF) while assuring a possibly wide bandwidth (the AD8610 were used). For other OPAMPs only AC parameters are important. The analysis of the influence of parameters A_{DC} and ω_{3dB} on the impedance measurement error was performed for two types of amplifiers: AD8610 (A_{DC} = 180000 ω_{3dB} = $2\pi \cdot$ 100 Hz) and AD8021 (A_{DC} = 25000 ω_{3dB} = $2\pi \cdot$ 50 kHz). Simulations were performed in the upper range of the measurement frequencies (>1 kHz), where the OPAMP's influence is the greatest (Fig. 5).
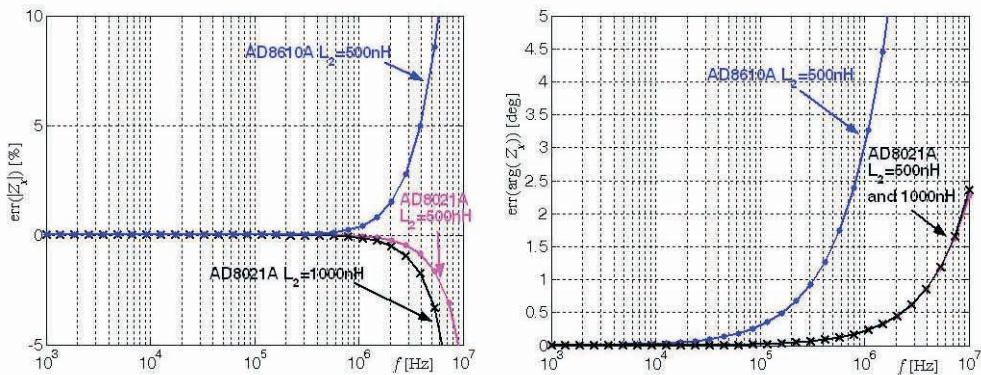

Fig. 5. Impedance modulus and argument measurement error caused by OPAMP parameter and cable inductance.

The analysis of the graphs shows that in case of different gains (1 and 0,1) in differential amplifiers, the impedance measurement error is much greater when using only AD8610. Because of this, in the probe, AD8610 amplifiers were used only as a voltage followers and the other amplifiers were based on AD8021. AC parameters of the amplifiers were taken into account in the formula for calculation of the measu-

red impedance, even they influence less the measurement error (when comparing to parasitic capacitance).

Figure 5 presents results of the simulations taking into account the influence of the inductance of the current cables (L_1 and L_2) on the error of the impedance measurement. For typical cables (length of 30 cm and inductance of ca. 500 nH) the modulus error is less important when comparing to the influence of the AC parameters of the OPAMPs. But inductances L_1 and L_2 with capacitances C_1 and C_3 create voltage dividers, which decrease the voltage across Z_x and R_R (Fig. 6). To eliminate this unwanted phenomenon, the analyzer automatically compensates the voltage across Z_x to a programmed value.
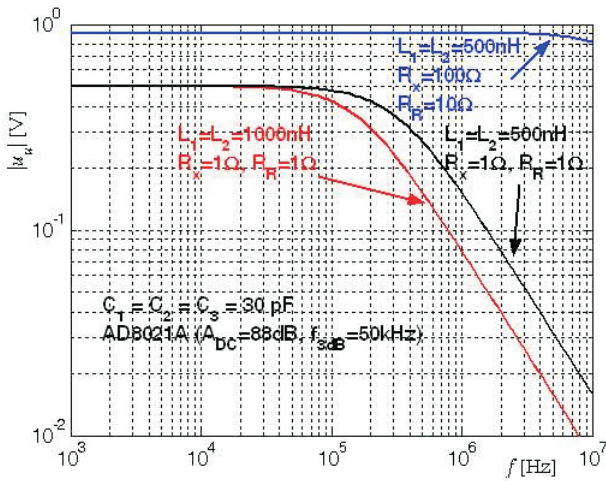

Fig. 6. Voltage signal u_u amplitude drop due to inductance of the cables.

3.3. Correction of the measurement results

The performed analysis of the probe showed that the signals u_i and u_u are affected also by unwanted parameters (*e.g.* parasitic capacitances, real-life parameters of the OPAMPs) causing errors in the measured impedance. Due to this, there is a need to enter corrections improving signals extracted in the probe. Using formula (1) taking into account the influence of all unwanted error sources, the formula for calculation of the measured impedance Z_x was written (for ranges $10\ \Omega \div 100\ \mathrm{M}\Omega$) as follows:

$$Z_x = \frac{U_u}{U_i}\frac{10\left(1+\frac{1,1}{A_u}\right)}{1+\frac{2}{A_u}}\left\{\left[j\omega C_2\left(j\omega L_2 + \frac{1}{j\omega C_3 + \frac{1}{R_R}}\right)\right]\left(j\omega C_3 + \frac{1}{R_R}\right)\right\}^{-1}. \qquad (2)$$

When measuring impedance below 10 Ω, in the formula (2) the ratio of coefficients containing OPAMPs parameter A_u is equal to 1, because the paths for voltage u_u and current u_i signals have the same gains for the lowest impedance range. The use of correction formula (2) allows to calculate the measured impedance with greater accuracy. Figs 7 and 8 show profits appearing when using formula (2) for calculation of modulus and argument of Z_x.

The influence of the parasitic capacitances is the greatest in case of high impedance measurements. So, Fig. 7 presents results of simulation using formula (2) for a RC two-terminal network consisting of parallel connection of R_x = 10 kΩ and C_x = 1 pF.
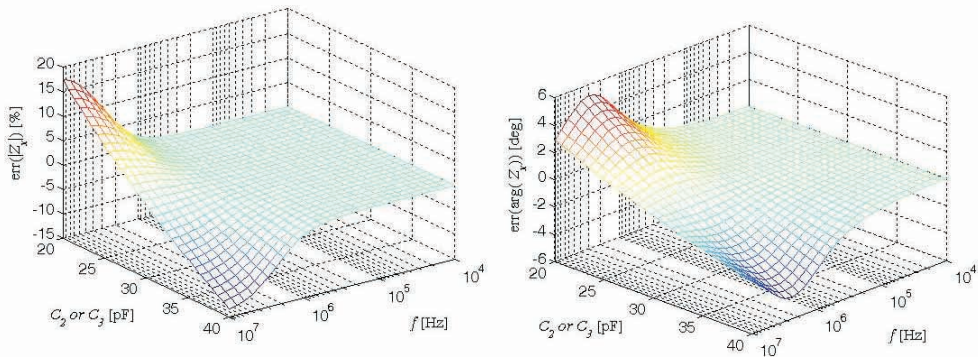

Fig. 7. Measurement error of impedance modulus and argument caused by non-precise elimination of C_2 or C_3 capacitance influence.

When analyzing graphs, a meaningful decrease of the measurement error can be noted when the real value of parasitic capacitance is used in formula (2) (in case of Fig. 7 it is equal to 30 pF). A similar effect can be obtained using the real value of inductance. Because the influence of the cable inductance can be seen only when measuring low impedance, in Fig. 8 the measurement of impedance is analyzed with modulus equal to 100 Ω. For inductance equal to 500 nH, corresponding with the real value inductance of the cable with a length of 25 cm, a correction of the measurement result takes place, significantly reducing errors of the modulus and argument of the measured impedance.
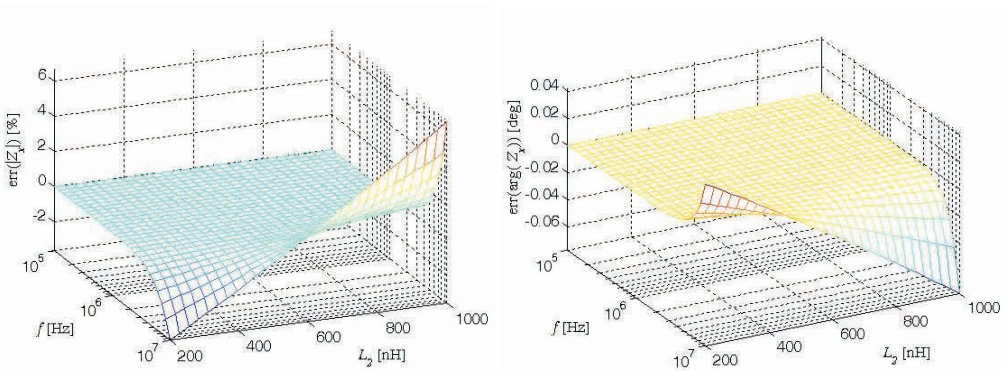
Fig. 8. Measurement error of impedance modulus and argument caused by non-precise elimination of the influence of inductance L_2.

4. Determination of orthogonal parts of the measurement signals

The procedure of the determination of orthogonal parts of the measurement signals u_i and u_u using DFT was described in [4]. The high impedance analyzer was using a quartz oscillator with a base frequency of 6,5536 MHz, what assures synchronous generation and acquisition for signals at frequencies up to 1,6384 MHz (4 samples per period, 65536 samples). The first step of the modification of the low-impedance analyzer towards increasing the measurement frequency was replacement of the quartz oscillator clocking generation to f_{quartz} = 32,768 MHz, which allows to achieve the required maximal measurement frequency equal to 10 MHz (ca. 3 samples per period). While dividing the clock frequency by 5 ($f_{quartz}/5$ = 6,5536 MHz), the previous solution was preserved for frequencies below 1 MHz. Frequency f_{quartz} is acceptable for DAC (LTC1668 f_{smax} = 50 MSps), but unfortunately it is too high for ADCs (LTC1420 f_{smax} = 10 MSps). Happily the bandwidth of the input circuitry of the ADCs (full-power bandwidth = 100 MHz) makes it possible use them to undersample signals [7].

For frequencies below 1,6384 MHz the previous method of generation/sampling based on identical sampling frequency is used for signal generation and acquisition of response signals. For higher frequencies, it was necessary to separate (logically – inside CPLD) signal clocking DAC (CLK2) and associated memory RAM2 (STROBE2) from signal clocking ADCs (CLK0_1) and associated memories RAM0 and RAM1 (STROBE0 and STROBE1). The above-listed signals are prepared in CPLD chip on the basis of signal f_{quartz}, which allows to preserve synchronous sampling. In Fig. 9, an example of sampling the signal at a frequency of 1,5 MHz (continuous line) using a sampling frequency of 6,5536 MHz (dots) and sampling frequency 1,6384 MHz (squares connected with line) was shown.
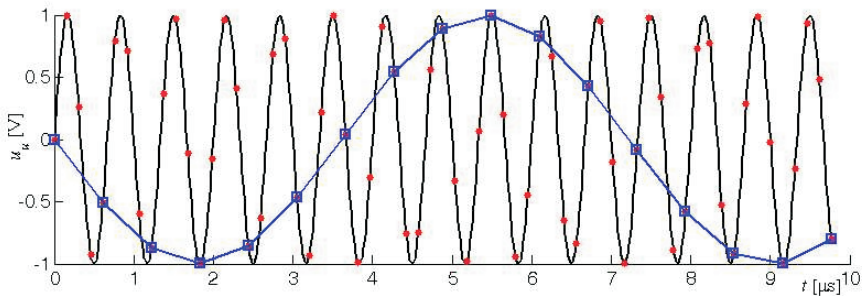
Fig. 9. Illustration of undersampling process.

Table 1 contains the division of frequency range above 1,6384 MHz to subranges with associated sampling frequencies. From previous subranges only the highest one containing 1 MHz frequency was shown in row 1. In column 2, the measurement frequency programming step was given. It results from the frequency clocking DAC and the number of samples of sinusoidal signal in memory RAM2 (65536). Column 4 shows the way of obtaining the sampling frequency by division of f_{quartz}.

When using undersampling, we use the shift of the sampled frequency by sampling frequency (effectively the difference f_{meas}-f_{sample} or f_{sample}-f_{meas} is sampled). For example, using the second row from Table 1, f_{sample} = 1,6384MHz, taking f_{meas} = 1,6385 MHz we obtain the difference f_{meas}-f_{sample} = 100 Hz. As a result in samples memory, the sinusoidal signal with imaginary frequency 100 Hz, and taking into account the resolution of the DFT DFT (25 Hz) - non-zero will be 4 line (4*25Hz = 100 Hz) and for this line the DSP calculates values of transforms of u_u and u_i.

Table 1. Measurement frequency ranges and assigned sampling frequencies.

f_{gen} (f_{meas}) [MHz]	Step Δf_{gen} [Hz]	f_{sample} [MHz]	f_{sample} source	Spectrum resolution [Hz]	Method
<=1.6384	100	6.5536	f_{quartz}/5	100	Sampling
1.6385–2.048	500	1.6384	f_{quartz}/20	25	Undersampling
2.0485–2.56	500	2.048	f_{quartz}/16	31.25	Undersampling
2.565–4.096	500	3.2768	f_{quartz}/10	50	Undersampling
4.0965–5.12	500	4.096	f_{quartz}/8	62.5	Undersampling
5.125–8.192	500	6.5536	f_{quartz}/5	100	Undersampling
8.1925–10.24	500	8.192	f_{quartz}/4	125	Undersampling

5. Experimental results

In order to verify the results of simulation, the measurements were performed using the realized probe and the analyser. As test objects connected to the input terminals of the probe, reference resistors with values: 10 Ω, 1 kΩ, 100 k and 10 MΩ were used. The values of the objects were measured with precise instrument RLC E4980A from Agilent. The measurements were performed at frequencies in the range of 10 Hz ÷ 10 MHz (with 1-2-5 step) using a signal with 1 V_{rms} amplitude. Figure 10 presents the measurement errors calculated from the results of the measurement of the modulus and argument of the impedance in two cases: without corrections and when applying the correction using formula (2).

When analyzing graphs (for the measured resistors 10 MΩ, 100 kΩ, 1 kΩ) a significant influence of parasitic capacitance on the error of impedance measurement can be noted when exceeding a specific measurement frequency, different for each range resistor. For range resistor R_R = 1 MΩ (measurement of 10 MΩ) the limit frequency is equal to 100 Hz in case of modulus and 10 Hz in case of argument of the impedance, and for R_R = 10 kΩ (measurement of 100 kΩ) respectively 10 kHz and 1 kHz. When applying a correction based on formula (2), the limiting frequencies are increased by a factor above 10, as shown in Fig. 10.
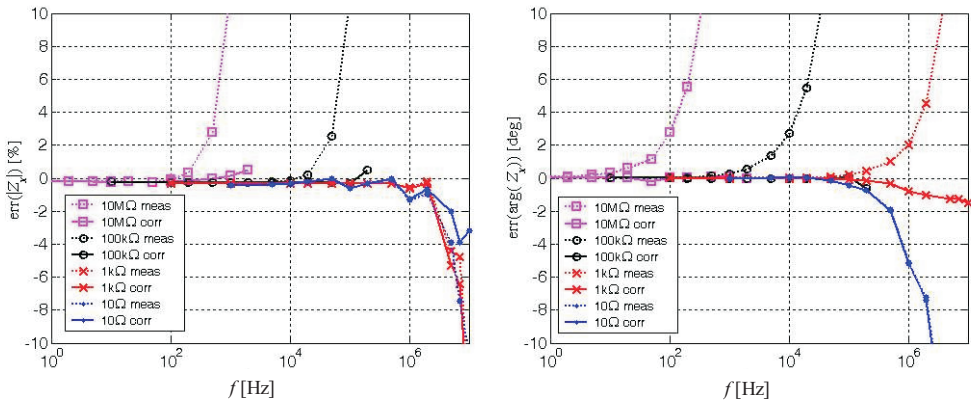
Fig. 10. Measurement errors for the test objects.

The influence of the parasitic capacitance in case of the measurement of the impedance below 1 kΩ (R_R = 100 Ω and 10 Ω) is much lower. For frequencies above 1 MHz, the AC parameters of OPAMPs and the inductance of terminals are most influencing the accuracy. For the measurement of low impedances ($|Z_x| \le$ 100Ω) at frequencies above 1 MHz, an additional coefficient influencing on the measurement error is the reference resistor which is not ideal. Due to this, the errors presented in Fig. 10, cannot be corrected adequately in this frequency range.

6. Conclusions

The realized analyzer for low-impedance spectroscopy, thanks to the use of the input circuitry in the form of a 5-terminal probe, allows impedance measurements in the range of 1 Ω <$|Z_x|$≤ 100 MΩ (in 8 subranges). To determine the orthogonal parts of the measurement signals the DSP technique was used, allowing to measure in a wide frequency range from 1 mHz up to 10 MHz (above 1 MHz undersampling technique was used).

The analysis of the probe was performed allowing to evaluate the accuracy of the impedance measurement. It was noticed that the error of the impedance modulus and argument is highly influenced by the parasitic capacitance existing in parallel to the range resistor in case of the impedance measurement with $|Z_x|$≥ 1 kΩ and by the parameters of the transfer function of the OPAMPs in case of high frequency range above 100 kHz. The comparison of simulation and measurement results of the realized probe has proved that the assumed equivalent circuit correctly reflects real-life parameters of the probe. This led to the correction formula, which allows to extend by one decade the maximal measurement frequency for ranges where the impedance modulus is greater than 1 kΩ. The elaborated formula, increasing measurement accuracy, was implemented in the PC software controlling the analyzer.

The presented solution of the impedance analyzer was sold to Electronic Systems Manufacture ATLAS – SOLLICH in Gdansk on the basis of a licence (no BTT/1/2009/L) in order to put the analyzer to production.

References

[1] J.L. Huertas: *Test and Design-for-Testability in Mixed-Signal Integrated Circuits*, Kluwer Academic Publishers, Boston, 2004.

[2] K. Arabi, B. Kaminska: "Oscillation-Test Methodology for Low-Cost Testing of Active analog Filters". *IEEE Transactions on Instrumentation and Measurement*, vol. 48, no. 4, 1999, pp. 798–806.

[3] D. Vazquez, G. Huertas, g. Leger, E. Peralias, A. Rueda, J.L. Huertas: "On-Chip Evaluation of Oscillation-Based-Test Output Signals for Switched – Capacitors Circuits". *Analog Integrated Circuits and Signal Processing*, vol. 33, 2002, pp 201–211.

[4] J. Hoja, G. Lentka.: "Virtual instrument using bilinear transformation for parameter identification of high impedance objects". *Meas. Sci. Tech.*, vol. 14, no 5, 2003, pp. 633–642.

[5] J. Hoja, G. Lentka: "An analysis of a measurement probe for a high impedance spectroscopy analyzer". *Measurement*, vol. 41, no. 1, pp. 65–75, 2008.

[6] S. Franco: *Operation amplifiers and analog integrated circuits*. McGraw-Hill Book Company, 1988.

[7] R.G. Lyons: *Understanding Digital Signal Processing*, Addison Wesley Longman Inc., 1997.